Phase behavior of dipolar fluids from a modified statistical associating fluid theory for potentials of variable range

Honggang Zhao and Clare McCabe[a)]
Department of Chemical Engineering, Vanderbilt University, Nashville, Tennessee 37235

(Received 8 May 2006; accepted 25 July 2006; published online 11 September 2006)

A statistical associating fluid theory for potentials of variable range to model dipolar fluids is presented. The new theory, termed the SAFT-VR+D equation (the statistical associating fluid theory for potentials of variable range plus dipole), explicitly accounts for dipolar interactions and their effect on the structure of the fluid. This is achieved through the use of the generalized mean spherical approximation (GMSA) to describe a reference fluid of dipolar square-well segments. Isothermal-isobaric and Gibbs ensemble Monte Carlo simulations have been performed in order to test the new theoretical approach. Predictions for the thermodynamic properties and phase behavior of dipolar square-well monomer and chain fluids, in which one or more segments are dipolar, are considered and compared with new computer simulation data. The results show that the equation of state in general provides a good description of the phase behavior of dipolar monomer and chain fluids. Some deviations are seen between the simulation data and theoretical predictions for monomer fluids with large dipole moments and for molecules composed of segments with dipoles in different orientations. This is addressed through the replacement of the GMSA by the linearized exponential approximation. © *2006 American Institute of Physics*. [DOI: 10.1063/1.2337624]

I. INTRODUCTION

Anisotropic interactions can have a significant effect on the thermodynamic properties of fluids, both for fluids of simple spherical molecules such as water to chainlike molecules such as alcohols and ketones. While many equations of state have been used to describe the thermodynamics of these systems, they often rely on effective parameters to describe the molecular interactions, and so have limited applicability beyond the fluids and state conditions to which the parameters were fitted. In order to develop a truly predictive approach for the thermophysical properties and phase behavior of fluids, the molecular-level interactions need to be explicitly included into the equation of state. For nonpolar fluids several molecular-based equations of state, such as the perturbed hard chain theory and the statistical associating fluid theory (SAFT), have been proposed in the literature. They have parameters that directly relate to molecular-level physical interactions. Perhaps the most successful of these molecular-based equations of state (EOS) is the SAFT approach proposed by Chapman *et al.*[1] on the basis of Wertheim's thermodynamic perturbation theory (TPT).[2] An important feature of the SAFT theory is that it explicitly takes into account nonsphericity and association interactions and provides a powerful method for investigating the phase behavior of both nonassociating and associating chain fluids. In the SAFT framework, the free energy is written as the sum of four separate contributions:

$$\frac{A}{Nk_BT}=\frac{A^{\text{ideal}}}{Nk_BT}+\frac{A^{\text{mono.}}}{Nk_BT}+\frac{A^{\text{chain}}}{Nk_BT}+\frac{A^{\text{assoc.}}}{Nk_BT}, \tag{1}$$

where N is the number of molecules, k_B Boltzmann's constant, and T the temperature. A^{ideal} is the ideal free energy, $A^{\text{mono.}}$ the contribution to the free energy due to the monomer segments, A^{chain} the contribution due to the formation of bonds between monomer segments, and $A^{\text{assoc.}}$ the contribution due to association interactions. Hence, a SAFT fluid is a collection of monomers that can form covalent bonds; the monomers interact via repulsive and attractive (dispersion) forces, and, in some cases, association interactions. The many different versions of SAFT essentially correspond to different choices for the monomer fluid and different theoretical approaches to the calculation of the monomer free energy and structure. For an excellent overview the reader is directed to a recent review.[3] In this work we focus on the statistical associating fluid theory for potentials of variable range (SAFT-VR), which describes chain molecules formed from hard-core monomers with attractive potentials of variable range,[4,5] typically a square well. The SAFT-VR equation has been successfully used to describe the phase equilibria of a wide range of industrially important systems; for example, alkanes of low molecular weight through to simple polymers,[4,6] and their binary mixtures,[7,8] perfluoroalkanes,[9] hydrogen fluoride,[10] boron triflouride,[11] water,[12] refrigerant systems,[13] carbon dioxide,[8,10,14] and electrolyte solutions[15] have all been studied.

While the SAFT equation in its many variations has been applied to the study of polar fluids, the molecular interactions between the molecules are typically taken into account in an effective way through the segment size and energy parameters.[16–18] In SAFT equations of state that have been

[a)]Author to whom correspondence should be addressed. Electronic mail: c.mccabe@vanderbilt.edu

specifically developed for polar fluids, dipolar and/or quadrupolar interactions are generally incorporated through the addition of the corresponding terms to Eq. (1). For the dipolar term, both the μ-expansion proposed by Gubbins and Gray,[19] which describes the interaction of dipolar hard sphere fluids using an angular pair correlation function, and the more rapidly converging Padé approximation of Stell *et al.*[20] have been widely adopted. For example, Muller and Gubbins[17] applied the μ-expansion to describe water as a hard, spherical associating dipolar fluid within Wertheim's TPT theory, achieving good agreement with simulation and experimental data. In a SAFT-like equation of state for alkanols and water Xu *et al.*[18] applied a Padé approximation to describe dipole-dipole interactions.

A common feature of these equations of state is to treat nonspherical dipolar molecules as spherical dipolar fluids. As a result, the orientation of the dipolar interaction and the possibility of multiple polar sites within a molecule cannot be taken into account. In contrast, Jog and co-workers[21] developed a SAFT EOS for tangent hard sphere chains with dipoles on alternate segments. This approach was subsequently used by Tumakaka and Sadowski[22] to extend the perturbed chain (PC)-SAFT EOS to describe mixtures of nondipolar and polar molecules. Dominik *et al.*[23] later compared polar PC-SAFT in which the dipolar contribution of Jog is used with predictions using an alternate dipolar term due to Saager and Fischer,[24] and found that while both approaches yield similar results the parameters for the original polar PC-SAFT were more physically meaningful. More recently, Gross and Vrabec[25] developed a contribution for dipolar interactions based on third order perturbation theory, which uses simulation data for the vapor-liquid equilibria of the two-center Lennard-Jones plus point dipole fluid to determine the model constants. The proposed term has been incorporated into the PC-SAFT equation of state and has been shown to improve the description of pure component and mixture phase equilibria for dipolar fluids over the original PC-SAFT approach.[25]

We note that in the SAFT EOS approaches summarized above, and to the best of our knowledge, in those reported in the literature to date, the inclusion of dipolar contributions to the equation of state has been limited to adding a dipolar term to the free energy, and therefore the structural impact of the dipolar interactions on the thermodynamics and phase behavior has not been considered.

An alternative approach to using perturbation theory to describe dipolar fluids is through integral-equation theory. Wertheim[26] solved the Ornstein-Zernike (OZ) equation using the mean spherical approximation (MSA) closure for dipolar hard spheres and provided analytical expressions for the thermodynamic and structural properties of the model. Patey and Valleau[27] and Verlet and Weis[28] subsequently performed computer simulations for the dipolar hard sphere system and found that the theoretical MSA harmonic coefficients for dipolar spheres are in good agreement with simulation data far from contact, but are too small at contact. Extensions, such as the optimized random phase approximation[29] (ORPA) and the exponential (EXP) approximation,[27] have been proposed to systematically improve the results of the MSA for the pair correlation function of dipolar hard spheres. In particular, the linearized version of the EXP (LEXP), suggested by Verlet and Weis,[28] provides considerable improvement for the pair correlation function over the MSA result at contact. Subsequently, Adelman and Deutch,[30] in a similar approach to Wertheim, solved the OZ equation for simple polar mixtures, in which the components are restricted to have equal diameters but may have different dipole moments. Although other integral-equation theories for dipolar fluids, such as the reference hypernetted chain approximation of Patey and co-workers[31] are available, these do not provide analytical expressions and so require numerical solution methods.

Here, we present an equation of state to model chain molecules with one or multiple dipolar sites embedded in specific segments of the chain through a combination of the MSA theory for dipolar interactions and the SAFT-VR equation. We refer to the resulting theory and EOS as SAFT-VR+D. In our model, the dipolar square-well monomer fluid is chosen as the reference fluid within the framework of the SAFT approach. The potential of the reference state therefore consists of two parts: an isotropic square-well potential and an anisotropic dipolar potential, for which we use the MSA and the SAFT-VR equation, respectively. Although the solution of the MSA for dipolar fluids is approximate, it provides analytical expressions for the thermodynamic and structural properties, thus permitting the development of a SAFT-VR equation of state for dipolar fluids in which the effect of the dipole on the phase behavior is explicitly described in the monomer and chain terms and not simply treated as a perturbation at the level of the monomer. In this work, two specific systems are considered: molecules with a dipole moment embedded in each segment and molecules in which dipole moments are embedded in specific segments.

The remainder of the paper is organized as follows: In Sec. II we present the SAFT-VR+D model and theory for dipolar square-well fluids. In Sec. III, details of the molecular simulations performed are presented. Results for the phase behavior of pure dipolar square-well fluids are presented and compared with simulation results in Sec. IV. Finally, concluding remarks are made and future work is discussed in Sec. V.

II. MODEL AND THEORY

A. Pure chain fluids

We have developed an accurate equation of state to model dipolar square-well fluids through a combination of the SAFT-VR approach and the generalized mean spherical approximation for dipolar fluids. As in the SAFT-VR approach, nonassociating molecules are described by four parameters: the size of the monomer segments σ, the depth ε and range λ of the square-well potential characterizing the attractive dispersion interactions between the monomer segments, and m which determines the number of segments tangentially bonded together in the model chain. The inclusion of dipolar interactions into the SAFT-VR EOS introduces three additional parameters: the dipole moment μ, and the

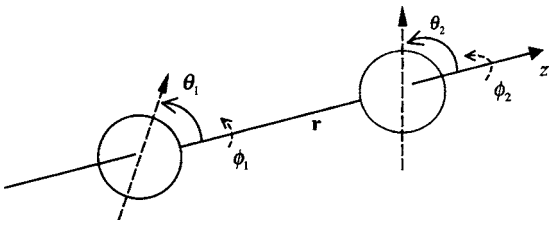

FIG. 1. The interdipole site coordinate system, with polar axis along r (Ref. 32).

orientation of the dipoles which is determined by the azimuthal θ, and polar ϕ angles of the intersegment axis along r, as shown in Fig. 1.[32]

In the SAFT-VR+D approach, the reference fluid is a dipolar square-well fluid with the dipole embedded in the center of the segment from which chain molecules of m tangentially bonded segments can be formed (Fig. 2). Each segment has a hard-core diameter σ and interacts through an intermolecular potential of the form

$$u(\mathbf{r}\boldsymbol{\omega}_1\boldsymbol{\omega}_2) = u^{\mathrm{HS}}(r,\sigma) - \varepsilon\phi^{\mathrm{SW}}(r;\lambda) + u^{\mathrm{dipole}}(\mathbf{r}\boldsymbol{\omega}_1\boldsymbol{\omega}_2). \quad (2)$$

Here, $\mathbf{r}$ is the vector between the center of the two monomers, $r=|\mathbf{r}|$, and $\boldsymbol{\omega}_i=(\theta_i,\phi_i)$ is the set of angles defining the orientation of the dipole in monomer i (see Fig. 1). As in the SAFT-VR equation the monomer-monomer isotropic potential consists of a hard sphere repulsive interaction u^{HS}, defined by

$$u^{\mathrm{HS}}(r;\sigma) = \begin{cases} \infty, & r < \sigma \\ 0, & r > \sigma, \end{cases} \quad (3)$$

and an attractive square-well interaction of depth $-\varepsilon$ and shape $\phi^{\mathrm{SW}}(r;\lambda)$, where λ is a parameter associated with the range of the attractive forces, viz.,

$$\phi^{\mathrm{SW}}(r;\lambda) = \begin{cases} 1, & \sigma < r < \lambda\sigma \\ 0, & r > \lambda\sigma. \end{cases} \quad (4)$$

The dipole-dipole potential is a long-range anisotropic interaction, which can be expressed as,

$$u^{\mathrm{dipole}}(\mathbf{r}\boldsymbol{\omega}_1\boldsymbol{\omega}_2) = -\frac{\mu^2}{r^3} D(\mathbf{n}_1\mathbf{n}_2\hat{\mathbf{r}}), \quad (5)$$

where

$$D(\mathbf{n}_1\mathbf{n}_2\hat{\mathbf{r}}) = 3(\mathbf{n}_1\cdot\hat{\mathbf{r}})(\mathbf{n}_2\cdot\hat{\mathbf{r}}) - \mathbf{n}_1\cdot\mathbf{n}_2. \quad (6)$$

Here $\hat{\mathbf{r}}$ is the unit vector in the direction of $\mathbf{r}$ joining the center of the segments (Fig. 1) and $\mathbf{n}_i$ is a unit vector parallel to the dipole moment of segment i.

Within the SAFT framework, the Helmholtz free energy A for N chains formed from m spherical segments, which in this work refers to spherical dipolar square-well segments, can be written in the form

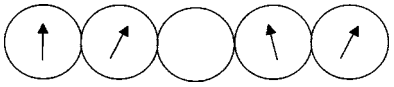

FIG. 2. Schematic illustrating the molecular model used to describe a chain fluid with dipole moments embedded in some or all segments.

$$\frac{A}{Nk_BT} = \frac{A^{\mathrm{ideal}}}{Nk_BT} + \frac{A^{\mathrm{mono}}}{Nk_BT} + \frac{A^{\mathrm{chain}}}{Nk_BT}, \quad (7)$$

where $A^{\mathrm{mono.}}$ is now the contribution due to the free energy due to the dipolar square-well monomer segments and A^{chain} represents the free energy due to chain formation from these segments and so explicitly includes the effect of the dipole interactions on the structure of the fluid. We have not included the contribution due to association interactions, as only nonassociating (i.e., hydrogen-bond-type association interactions) dipolar chain molecules are considered in this first extension of the theory.

In order to understand the nature of the MSA solution and its relevance to the current problem, we need to examine it briefly. The MSA for dipolar hard spheres arises from the exact Ornstein-Zernike equation for linear molecules, given by

$$h(\mathbf{r}\boldsymbol{\omega}_1\boldsymbol{\omega}_2) = c(\mathbf{r}\boldsymbol{\omega}_1\boldsymbol{\omega}_2) + \frac{\rho}{4\pi} \times \int h(\mathbf{r}_{12}\boldsymbol{\omega}_1\boldsymbol{\omega}_3)c(\mathbf{r}_{23}\boldsymbol{\omega}_3\boldsymbol{\omega}_2)d\mathbf{r}_3 d\boldsymbol{\omega}_3, \quad (8)$$

where $h(\mathbf{r}\boldsymbol{\omega}_1\boldsymbol{\omega}_2)$ and $c(\mathbf{r}\boldsymbol{\omega}_1\boldsymbol{\omega}_2)$ are the total and direct correlation functions, respectively. The total correlation function is related to the pair distribution function $g(\mathbf{r}\boldsymbol{\omega}_1\boldsymbol{\omega}_2)$ by $h(\mathbf{r}\boldsymbol{\omega}_1\boldsymbol{\omega}_2)=g(\mathbf{r}\boldsymbol{\omega}_1\boldsymbol{\omega}_2)-1$. The MSA closure for a hard-core potential states that

$$\begin{aligned} h(\mathbf{r}\boldsymbol{\omega}_1\boldsymbol{\omega}_2) &= -1, \quad r < \sigma, \\ c(\mathbf{r}\boldsymbol{\omega}_1\boldsymbol{\omega}_2) &= -\frac{1}{k_BT} u(\mathbf{r}\boldsymbol{\omega}_1\boldsymbol{\omega}_2), \quad r > \sigma. \end{aligned} \quad (9)$$

Hence, the MSA for dipolar hard spheres becomes

$$\begin{aligned} h(\mathbf{r}\boldsymbol{\omega}_1\boldsymbol{\omega}_2) &= -1, \quad r < \sigma, \\ c(\mathbf{r}\boldsymbol{\omega}_1\boldsymbol{\omega}_2) &= \frac{\mu^2}{k_BTr^3} D(\mathbf{n}_1\mathbf{n}_2\hat{\mathbf{r}}), \quad r > \sigma. \end{aligned} \quad (10)$$

Wertheim[26] showed that with this closure the total and direct correlation functions for dipolar hard spheres in the MSA can be written in the following simplified forms

$$\begin{aligned} h(\mathbf{r}\boldsymbol{\omega}_1\boldsymbol{\omega}_2) &= h_s(r) + h_\Delta(r)\Delta(\mathbf{n}_1\mathbf{n}_2) + h_D(r)D(\mathbf{n}_1\mathbf{n}_2\hat{\mathbf{r}}), \\ c(\mathbf{r}\boldsymbol{\omega}_1\boldsymbol{\omega}_2) &= c_s(r) + c_\Delta(r)\Delta(\mathbf{n}_1\mathbf{n}_2) + c_D(r)D(\mathbf{n}_1\mathbf{n}_2\hat{\mathbf{r}}), \end{aligned} \quad (11)$$

where $\Delta(\mathbf{n}_1\mathbf{n}_2)=\mathbf{n}_1\cdot\mathbf{n}_2$; $h_s(r)$, $h_\Delta(r)$, $h_D(r)$, and the corresponding direct correlation quantities are functions of r only. Moreover, within the MSA, $h_s(r)$ and $c_s(r)$ are given by their Percus-Yevick (PY) hard sphere values, and $h_\Delta(r)$ and $h_D(r)$ are calculated from functions arising from the solution of the PY approximation for hard spheres. We point out, however, that much of the Wertheim solution holds true in more general cases. For example, consider the dipolar square-well fluid in the generalized MSA (GMSA):[33]

$$h(\mathbf{r}\boldsymbol{\omega}_1\boldsymbol{\omega}_2) = -1, \quad r < \sigma,$$
$$c(\mathbf{r}\boldsymbol{\omega}_1\boldsymbol{\omega}_2) = c^{\mathrm{SW}}(r) + \frac{\mu^2}{k_B T r^3} D(\mathbf{n}_1\mathbf{n}_2\hat{\mathbf{r}}), \quad r > \sigma, \tag{12}$$

where $c^{\mathrm{SW}}(r)$ is the direct correlation for the square-well fluid (i.e., the usual, nondipolar square-well fluid). With this GMSA closure, the solution of the Ornstein-Zernike equation is given by

$$h^{\mathrm{DSW}}(\mathbf{r}\boldsymbol{\omega}_1\boldsymbol{\omega}_2) = h^{\mathrm{SW}}(r) + h_\Delta(r)\Delta(\mathbf{n}_1\mathbf{n}_2) + h_D(r)D(\mathbf{n}_1\mathbf{n}_2\hat{\mathbf{r}}),$$
$$c^{\mathrm{DSW}}(\mathbf{r}\boldsymbol{\omega}_1\boldsymbol{\omega}_2) = c^{\mathrm{SW}}(r) + c_\Delta(r)\Delta(\mathbf{n}_1\mathbf{n}_2) + c_D(r)D(\mathbf{n}_1\mathbf{n}_2\hat{\mathbf{r}}), \tag{13}$$

where now $h^{\mathrm{SW}}(r)$ and $c^{\mathrm{SW}}(r)$ are the correlation functions for the square-well fluid and $h_\Delta(r)$ and $h_D(r)$ are again obtained in terms of hard sphere Percus-Yevick quantities. This is because the GMSA closure on these quantities is the same as that for the MSA dipolar hard sphere case, namely,

$$h_\Delta(r) = 0, \quad r < \sigma,$$
$$h_D(r) = 0, \quad r < \sigma,$$
$$c_\Delta(r) = 0, \quad r > \sigma,$$
$$c_D(r) = \frac{\mu^2}{k_B T r^3}, \quad r > \sigma. \tag{14}$$

Note that $h^{\mathrm{SW}}(r)$ and $c^{\mathrm{SW}}(r)$ can be the exact such quantities or those calculated by some approximate theory (such as perturbation theory). Hence, within the GMSA, the pair distribution function $g^{\mathrm{DSW}}(\mathbf{r}\boldsymbol{\omega}_1\boldsymbol{\omega}_2)$ and Helmholtz free energy of dipolar square-well monomers are given by

$$g^{\mathrm{DSW}}(\mathbf{r}\boldsymbol{\omega}_1\boldsymbol{\omega}_2;\rho,T) = g^{\mathrm{SW}}(r;\rho,T) + h_\Delta(r;\rho,T)\Delta(\mathbf{n}_1\mathbf{n}_2) + h_D(r;\rho,T)D(\mathbf{n}_1\mathbf{n}_2\hat{\mathbf{r}}),$$
$$A^{\mathrm{DSW}}(r;\rho,T) = A^{\mathrm{SW}}(r;\rho,T) + A^{\mathrm{dipole}}(\mathbf{r}\boldsymbol{\omega}_1\boldsymbol{\omega}_2;\rho,T), \tag{15}$$

where $g^{\mathrm{SW}}(r)$ is the radial distribution function of the square-well monomer fluid and the state dependence of the quantities on ρ and T is explicitly shown. Detailed expressions for each term of the equation of state are presented below.

1. Ideal contribution

The free energy of an ideal gas is given by

$$\frac{A^{\mathrm{ideal}}}{Nk_BT} = \ln(\rho\Lambda^3) - 1, \tag{16}$$

where $\rho = N/V$ is the number density of chain molecules, N the number of molecules, V the volume of the system, and Λ the thermal de Broglie wavelength. Since the ideal term is separated out, the remaining terms are noted as residual free energies.

2. Monomer contribution

The contribution to the Helmholtz free energy due to the monomer segments is

$$\frac{A^{\mathrm{mono}}}{Nk_BT} = m\frac{A^{\mathrm{mono}}}{N_s k_B T} = ma^M, \tag{17}$$

where N_s is the total number of dipolar spherical monomers. Within the GMSA the excess Helmholtz free energy per monomer a^M is given by

$$a^M = a^{\mathrm{DSW}} = a^{\mathrm{dipole}} + a^{\mathrm{isotropic}},$$

where a^{dipole} describes the contribution to the free energy due to the anisotropic dipolar interaction. Within the high-temperature perturbation theory of Barker and Henderson, in the inverse of the temperature $\beta = 1/k_BT$, the isotropic term $a^{\mathrm{isotropic}}$ is given by

$$a^{\mathrm{isotropic}} = a^{\mathrm{HS}} + \beta a_1^{\mathrm{SW}} + \beta^2 a_2^{\mathrm{SW}}.$$

Hence

$$a^M = a^{\mathrm{dipole}} + a^{\mathrm{HS}} + \beta a_1^{\mathrm{SW}} + \beta^2 a_2^{\mathrm{SW}}. \tag{18}$$

The isotropic contribution to the free energy is expressed as in the SAFT-VR approach by a^{HS}, the free energy due to repulsive interactions between the hard cores, and a_1^{SW} and a_2^{SW}, the first and second perturbative terms associated with the isotropic attractive energy. The expression of Carnahan and Starling is used for the hard sphere term,

$$a^{\mathrm{HS}} = \frac{4\eta - 3\eta^2}{(1-\eta)^2}, \tag{19}$$

where η is the packing fraction, defined as $\eta = (\pi/6)\rho_s\sigma^3$. The first perturbative term of the mean attractive energy corresponds to the average of the monomer-monomer interaction calculated with the hard sphere structure. Using the mean-value theorem, we can obtain an expression for a_1^{SW} in terms of an effective packing fraction η_{eff} evaluated at contact,[34]

$$a_1^{\mathrm{SW}} = -4\eta\varepsilon(\lambda^3 - 1)g^{\mathrm{HS}}(1;\eta_{\mathrm{eff}}), \tag{20}$$

where the Carnahan and Starling equation of state is used to evaluate $g^{\mathrm{HS}}(1;\eta_{\mathrm{eff}})$.

$$g^{\mathrm{HS}}(1;\eta_{\mathrm{eff}}) = \frac{1 - \eta_{\mathrm{eff}}/2}{(1-\eta_{\mathrm{eff}})^3}. \tag{21}$$

For the range $1.1 \leqslant \lambda \leqslant 1.8$, the effective packing fraction η_{eff} is described by a function of η and λ, viz.,

$$\eta_{\mathrm{eff}}(\eta,\lambda) = c_1\eta + c_2\eta^2 + c_3\eta^3, \tag{22}$$

where the coefficients c_n are given by

$$\begin{pmatrix} c_1 \\ c_2 \\ c_3 \end{pmatrix} = \begin{pmatrix} 2.258\,55 & 0.249\,434 & 0.249\,434 \\ -0.669\,270 & -0.827\,739 & -0.827\,739 \\ 10.157\,6 & 5.308\,27 & 5.308\,27 \end{pmatrix} \times \begin{pmatrix} 1 \\ \lambda \\ \lambda^2 \end{pmatrix}. \tag{23}$$

The second perturbation term a_2^{SW} is obtained from the first density derivative of a_1^{SW} within the local compressibility approximation,

$$a_2^{\mathrm{SW}} = \frac{1}{2}\varepsilon K^{\mathrm{HS}} \eta \frac{\partial a_1^{\mathrm{SW}}}{\partial \eta}, \tag{24}$$

where K^{HS} is the hard sphere isothermal compressibility of PY

$$K^{\mathrm{HS}} = \frac{(1-\eta)^4}{1+4\eta+4\eta^2}. \tag{25}$$

The contribution to the free energy due to the dipolar interaction is obtained from Wertheim's solution of the Ornstein-Zernike equation for dipolar hard spheres with the MSA closure as given by Eq. (10);[26] the excess free energy due to the dipolar interactions is given by

$$a^{\mathrm{dipole}} = -\frac{8}{\eta}\xi^2\left[\frac{(1+\xi)^2}{(1-2\xi)^4} + \frac{(2-\xi)^2}{8(1+\xi)^4}\right], \tag{26}$$

where $\xi = \kappa\eta$ and κ is the scaling parameter. κ is determined by y, the so-called strength of the dipolar effect,[26]

$$3y = q_{\mathrm{PY}}(k\eta) - q_{\mathrm{PY}}(-\kappa\eta), \tag{27}$$

and is a dimensionless function of density ρ, temperature β, and dipole moment μ,

$$y = \frac{4\pi}{9}\rho\beta\mu^2. \tag{28}$$

q_{PY} is the dimensionless inverse compressibility of PY, given by[26]

$$q_{\mathrm{PY}}(\eta) = \frac{(1+2\eta)^2}{(1-\eta)^4}. \tag{29}$$

3. Chain contribution

The contribution to the free energy due to chain formation from m dipolar square-well monomer segments is given by

$$\frac{A^{\mathrm{chain}}}{Nk_BT} = -(m-1)\ln y^{\mathrm{DSW}}(\sigma\boldsymbol{\omega}_1\boldsymbol{\omega}_2), \tag{30}$$

where $y^{\mathrm{DSW}}(\sigma\boldsymbol{\omega}_1\boldsymbol{\omega}_2)$ is the dipolar square-well monomer background correlation function evaluated at hard-core contact,

$$y^{\mathrm{DSW}}(\mathbf{r}\boldsymbol{\omega}_1\boldsymbol{\omega}_2;\rho,T) = \exp[\beta u^{\mathrm{DSW}}(\mathbf{r}\boldsymbol{\omega}_1\boldsymbol{\omega}_2)]g^{\mathrm{DSW}}(\mathbf{r}\boldsymbol{\omega}_1\boldsymbol{\omega}_2;\rho,T), \tag{31}$$

where $g^{\mathrm{DSW}}(\mathbf{r}\boldsymbol{\omega}_1\boldsymbol{\omega}_2;\rho,T)$ is the pair distribution function for the dipolar square-well fluid and is obtained from GMSA [Eq. (15)]. In the SAFT-VR equation, a high-temperature perturbation expansion is used to determine the radial distribution function for the square-well fluid $g^{\mathrm{SW}}(r)$,

$$g^{\mathrm{SW}}(r) = g^{\mathrm{HS}}(r) + \beta\varepsilon g_1(r), \tag{32}$$

where the radial distribution function $g^{\mathrm{SW}}(r)$ at hard-core contact is given by

$$g^{\mathrm{SW}}(\sigma^+) = g^{\mathrm{HS}}(\sigma) + \beta\varepsilon g_1(\sigma), \tag{33}$$

where $g_1(\sigma)$ can be obtained from a self-consistent calculation of the pressure using the Clausius virial theorem and the first derivative of the free energy with respect to the density.

When compared with the Monte Carlo simulation data of Verlet and Weis,[28] Wertheim's solution of the OZ equation with the MSA closure underestimates the spherical harmonic coefficients at contact. As discussed in the Introduction, extensions such as ORPA, EXP, and LEXP have been suggested to improve the description of structural properties. Among them, the LEXP approximation is the most attractive; the LEXP $h_\Delta(r;\rho,T)$ and $h_D(r;\rho,T)$ appear the most accurate in comparison with simulation data, though the LEXP result for $h_s(r)$ shows little improvement over the MSA results. Within the LEXP approximation, the radial distribution function of the square-well monomer is given by

$$g^{\mathrm{DSW}}(\mathbf{r}\boldsymbol{\omega}_1\boldsymbol{\omega}_2;\rho,T) = g^{\mathrm{SW}}(r;\rho,T)(1 + h_\Delta(r;\rho,T)\Delta(\mathbf{n}_1\mathbf{n}_2) + h_D(r;\rho,T)D(\mathbf{n}_1\mathbf{n}_2\hat{\mathbf{r}})). \tag{34}$$

The spherical harmonic coefficients, $h_\Delta(r;\rho,T)$ and $h_D(r;\rho,T)$, can be obtained from the analytic solution of the PY approximation for the hard sphere fluid as

$$h_\Delta(r;\eta,T) = -2\kappa(h_{\mathrm{PY}}(-\kappa\eta,r) - h_{\mathrm{PY}}(2\kappa\eta,r)), \tag{35}$$

$$h_D(r;\eta,T) = \kappa\left(h_{\mathrm{PY}}(-\kappa\eta,r) + 2h_{\mathrm{PY}}(2\kappa\eta,r) - \int_0^r h_{\mathrm{PY}} \times(-\kappa\eta,r')dr' - 2\int_0^r h_{\mathrm{PY}}(2\kappa\eta,r')dr'\right).$$

We note that κ is a function of temperature, which is determined by the strength of the dipolar effect as given by Eq. (27)–(29). The spherical harmonic coefficient $h_{\mathrm{PY}}(\rho;r)$ is obtained by solving the OZ equation with the PY closure by introducing the dimensionless quantities $x = r/\sigma$ and $\bar{q}_{\mathrm{PY}}(x) = q_{\mathrm{PY}}(x)/\sigma^2$,

$$xh_{\mathrm{PY}}(x) = -\bar{q}'_{\mathrm{PY}}(x) + 12\eta\int_0^1 dx'\bar{q}_{\mathrm{PY}}(x')(x-x')h_{\mathrm{PY}}(|x - x'|), \tag{36}$$

for all $x \geq 0$, where $\bar{q}'_{\mathrm{PY}}(x) \equiv d\bar{q}_{\mathrm{PY}}(x)/dx$. $\bar{q}_{\mathrm{PY}}(x)$ is given by

$$\bar{q}_{\mathrm{PY}}(x) = \begin{cases} \frac{1}{2}a(x^2-1) + b(x-1), & x \leq 1 \\ 0, & x \geq 1. \end{cases} \tag{37}$$

For $x < 1$,

$$\bar{q}'_{\mathrm{PY}}(x) = ax + b, \tag{38}$$

where

$$a = \frac{1+2\eta}{(1-\eta)^2},$$

$$b = -\frac{3\eta}{2(1-\eta)^2}. \tag{39}$$

The analytic expression of $h_{\mathrm{PY}}(\rho;r)$ at contact can be obtained by setting $x = 1^+$ in Eqs. (36) and (37), giving

$$h_{\mathrm{PY}}(\eta,\sigma)=\frac{\eta(5-2\eta)}{2(1-\eta)^2}. \tag{40}$$

Both the LEXP approximation and GMSA are used in the SAFT-VR+D equation to determine the thermodynamic properties and phase behavior of the dipolar fluids studied from the Helmholtz free energy using standard thermodynamic relations.

B. Chains with mixed dipole moments

While the expressions given above treat chain molecules formed from dipolar square-well segments, each having the same dipolar strength, we can also consider chain molecules that contain segments with different strengths and orientations of dipole moments.

Adelman and Deutch[30] provided an exact solution to the MSA for simple polar mixtures with equal hard sphere radii and differing dipole moment, in which the structure and thermodynamic properties are completely determined from the pure dipolar fluid result of Wertheim using an effective density $\hat{\rho}$ and dipole moment $\hat{\mu}$. Substituting the effective density and dipole moment into Eq. (26) and (35), the Helmholtz free energy and radial distribution function due to dipolar interactions can easily be obtained for chain molecules with mixed dipole moments. The limiting case of chain molecules composed of a mixture of dipolar and nondipolar segments can also be studied. In their solution of the MSA Adelman and Deutch[30] determined that the pair correlation function of the nondipolar segments are unaffected by the presence of the dipoles on dipolar segments, and vice versa. This is a direct result of the linearity in the MSA approximation between the direct correlation function and the dipole-dipole interaction, as shown in Eq. (10). Hence, in the limiting case of a diatomic dipolar molecule in which the dipole moments of one and/or two of the segments μ_i and/or μ_j are zero, the anisotropic component of the direct correlation function of the dipolar hard sphere and nondipolar hard sphere is zero. Accordingly, within the GMSA, the pair distribution function $g^{\mathrm{DSW}}(\mathbf{r}\boldsymbol{\omega}_1\boldsymbol{\omega}_2)$ for a square-well diatomic molecule consisting of one dipolar segment (sphere 1) and one nondipolar segment (sphere 2) is reduced to the pair distribution function of nondipolar molecules $g^{\mathrm{SW}}(r)$ for three (g_{12},g_{21},g_{22}) out of the four possible pair correlation functions. Correspondingly, the Helmholtz free energy due to chain formation in the SAFT-VR+D EOS for chain molecules consisting of dipolar and nondipolar segments is given by

$$\frac{A^{\mathrm{chain}}}{Nk_BT}=-(m-m'-1)\ln y^{\mathrm{SW}}(\sigma)-\sum_{\text{bonded dipole pairs }ij}\ln y_{ij}^{\mathrm{DSW}}(\sigma\boldsymbol{\omega}_i\boldsymbol{\omega}_j), \tag{41}$$

where m' is the number of bonds between two dipolar spheres (i.e., equal to the number of terms in the sum). Hence, as in the hetero-SAFT-VR approach[35] the Helmholtz free energy directly reflects the structure of the chains through explicit dependence on the magnitudes and relative orientation of dipoles in neighboring dipolar segments.

III. COMPUTER SIMULATIONS

Monte Carlo simulations have been performed to study the thermodynamic properties of dipolar square-well monomer and chain fluids. The simulations were performed in both the isothermal-isobaric (*NPT*) and Gibbs (GEMC) ensembles. Intermolecular and nonbonded intramolecular interactions, except for nearest neighbors along the chain, are taken into account through the dipolar square-well potential given by Eq. (2). The reaction field[36,37] method, which has been shown to be adequate to calculate vapor-liquid phase behavior for systems with long-range dipolar potentials,[38] is applied to deal with the long-range dipolar interactions. The reaction field approach replaces the molecules beyond a cutoff distance by a dielectric continuum, the effect of which is taken into account by including a new term into the dipolar potential, viz.,[39]

$$u^{\mathrm{dipole}}=\begin{cases}-\left(\dfrac{\mu_1\mu_2}{r^3}\right)D-\dfrac{2(\varepsilon_{\mathrm{RF}}-1)}{2\varepsilon_{\mathrm{RF}}+1}\dfrac{\mu_1\mu_2}{r_c^3}, & r<r_c\\ 0, & r\geqslant r_c,\end{cases} \tag{42}$$

where r_c is the cutoff distance beyond which the pair potential vanishes and $\varepsilon_{\mathrm{RF}}$ the dielectric constant of the continuum. In the simulations reported here, the value of r_c is set to 2.5σ, and $\varepsilon_{\mathrm{RF}}$ to ∞. In both the *NPT* and GEMC simulations, the usual periodic boundary conditions and minimum image convention are used. In the *NPT* ensemble simulations, one cycle consists of three kinds of trial moves: *N* trial displacements of randomly chosen molecules, *N* trial rotations, and one volume change. The extent of each trial move is adjusted to give an individual acceptance probability of 30%–40%. In the GEMC simulations, particle exchanges between two phases are performed in addition to the three trial moves described above. The traditional Widom particle insertion method is used to achieve particle exchanges. Each simulation was started from an initial configuration in which 128 molecules are placed on a lattice in the simulation box. An initial simulation of 100 000–500 000 cycles was performed to equilibrate the system, before averaging for between 500 000 and 2 000 000 cycles. The thermodynamic properties of the system were obtained as ensemble averages and the errors estimated by determining the standard deviation.

Before studying the dipolar square-well fluids of interest in this work, to check the accuracy of our simulation code, we calculated the coexistence curve of several Stockmayer fluids using the GEMC technique and the reaction field method to treat the long-range dipolar interactions. Good agreement was obtained with the results of Smit *et al.*,[40] who accounted for the long-range dipolar interactions with the Ewald summation method.

IV. RESULTS AND DISCUSSION

We have studied the phase behavior of several dipolar square-well monomer fluids (systems 1–4), several dipolar diatomic fluids with a dipole moment in each segment, (systems 5–12), and dipolar triatomic fluids with one nondipolar

TABLE I. Model parameters for the dipolar square-well monomer and chain fluids studied.

System	ε^*	λ	σ^*	m	$(\mu_1^*)^2$	$(\mu_2^*)^2$	$(\mu_3^*)^2$
1	1	1.5	1	1	0.5	⋯	⋯
2	1	1.5	1	1	1.0	⋯	⋯
3	1	1.5	1	1	2.0	⋯	⋯
4	1	1.8	1	1	1.0	⋯	⋯
5	1	1.5	1	2	0.5[a]	0.5[a]	⋯
6	1	1.5	1	2	0.5[b]	0.5[b]	⋯
7	1	1.8	1	2	0.5[a]	0.5[a]	⋯
8	1	1.8	1	2	0.5[b]	0.5[b]	⋯
9	1	1.5	1	2	1.0[a]	0.5[a]	⋯
10	1	1.5	1	2	1.0[b]	0.5[b]	⋯
11	1	1.5	1	2	0.5[b]	0.5[a]	⋯
12	1	1.5	1	2	1.0[b]	1.0[a]	⋯
13	1	1.5	1	3	1.0[a]	1.0[a]	0.0
14	1	1.5	1	3	1.0[b]	1.0[b]	0.0

[a]Parallel dipole moments.
[b]Perpendicular dipole moments.

segment (systems 13 and 14). The details of these systems are listed in Table I. Comparisons are made between the theoretical predictions and *NPT* and Gibbs ensemble simulation data in order to validate and test the predictive ability of the SAFT-VR+D EOS for dipolar monomer and chain molecules. The numerical results of the *NPT* simulations are reported in Tables I–IV, and those of the GEMC simulations in Table V of the supplementary material.[41]

In Fig. 3, we present comparisons of the SAFT-VR+D predictions with molecular simulation results for the *PVT* behavior of monomer fluids with different dipole moments (systems 1–3). From the figure we see that the system with the highest reduced dipole moment (system 3) exhibits the highest density at a given pressure and temperature, as would be expected due to the increase in attractive interactions between the molecules. We observe good agreement between the simulation results and theoretical predictions over a wide range of temperatures and pressures for systems 1 and 2; however, the SAFT-VR+D EOS is seen to slightly underpredict the density at a given temperature and pressure for system 3, which has the highest value of the reduced dipole moment.

In order to obtain a more comprehensive understanding of the thermodynamic properties of the systems studied and further test the SAFT-VR+D approach, we also determined the fluid phase diagram for systems 1 and 2. The results are presented in Fig. 4 along with the phase diagram for a nondipolar square-well fluid with the same model parameters (i.e., $\varepsilon^*=1.0$, $\lambda=1.5$, and $\sigma^*=1.0$) for comparison. From the figure we see that as the dipole moment increases the critical temperature of the system increases, due to the increase in the attractive interactions. We also note from the figure that the SAFT-VR+D equation appears to overestimate the critical point; this is an unavoidable feature of equations of state such as SAFT that are based on analytical expressions for the free energy.[42] Away from the critical region we see good agreement between the theory and simulation for system 1 with the lowest dipole moment. For fluids with larger reduced dipole moments, we notice a slight disagreement between the SAFT-VR+D description and simulation data, particularly for the liquid density at low temperatures. Patey and Valleau[27] observed a similar trend in that the GMSA does not provide a good description of the thermodynamic properties of dipolar hard spheres with large dipole moments.

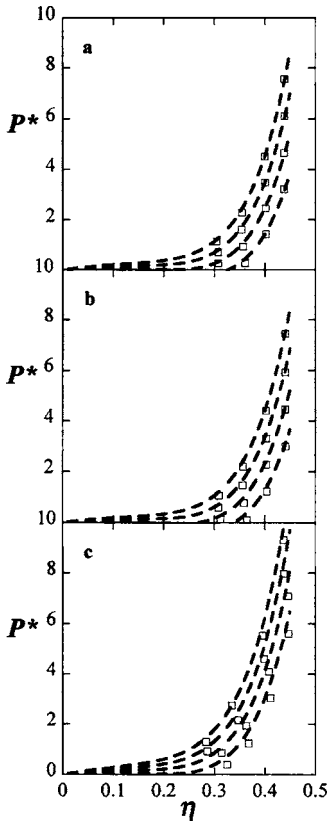

FIG. 3. Isotherms for dipolar square-well monomer fluids with $\varepsilon^*=1.0$, $\lambda=1.5$, $\sigma^*=1.0$, and (a) dipole moment $\mu^{*2}=0.5$ at $T^*=1.0$, 1.2, 1.4, and 1.6 (from bottom to top), (b) dipole moment $\mu^{*2}=1.0$ at $T^*=1.0$, 1.2, 1.4, and 1.6 (from bottom to top), and (c) dipole moment $\mu^{*2}=2.0$ at $T^*=1.4$, 1.6, 1.8, and 2.0 (from bottom to top). The dashed lines represent predictions from the SAFT-VR+D equation with the GMSA approximation and the squares the *NPT* MC simulation data.

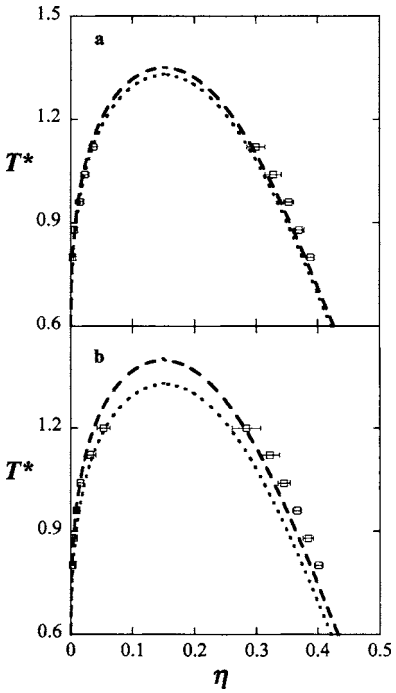

FIG. 4. Coexisting densities for dipolar square-well monomer fluids with $\varepsilon^*=1.0$, $\lambda=1.5$, $\sigma^*=1.0$, and dipole moment (a) $\mu^{*2}=0.5$ and (b) $\mu^{*2}=1.0$. The squares represent the GEMC simulation data, the dashed lines predictions from the SAFT-VR+D equation with the GMSA approximation, and the dotted lines predictions from the SAFT-VR+D equation for $\mu^{*2}=0$.

In the original development of the SAFT-VR EOS Gil-Villegas *et al.*[43] determined that SAFT-VR was in good agreement with GEMC simulation data for the vapor-liquid coexistence densities of square-well monomer fluids with potential ranges $1.1 \leqslant \lambda \leqslant 1.8$. In order to examine the effect of λ on the phase behavior of dipolar fluids and further test the SAFT-VR+D approach, we have studied the *PVT* behavior of the dipolar square-well monomer fluid with $\lambda=1.8$, $\sigma^*=1.0$, $\varepsilon^*=1.0$, and $\mu^{*2}=1.0$ (system 4) to compare to the results for system 2, for which $\lambda=1.5$ and with all other parameters the same. The results are presented in Fig. 5. Compared to the results for system 2 [Fig. 3(b)], we note that as λ increases, the density of the system increases at a given pressure and temperature. Good agreement is observed between the theoretical predictions and simulation data; the new SAFT-VR+D approach is seen to capture the effect of the potential range on the phase behavior.

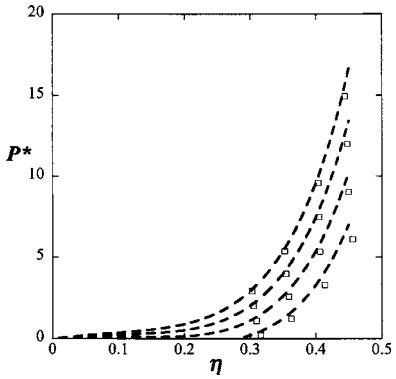

FIG. 5. Isotherms for dipolar square-well monomer fluids with $\varepsilon^*=1.0$, $\lambda=1.8$, $\sigma^*=1.0$, and dipole moment $\mu^{*2}=1.0$ at $T^*=1.6$, 2.0, 2.4, and 2.8 (from bottom to top). The squares represent *NPT* MC simulation results and the dashed lines predictions from the SAFT-VR+D equation with the GMSA approximation.

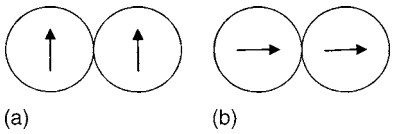

FIG. 6. Schematic model for diatomic dipolar fluids with dipole moments embedded in every segment (a) perpendicular and (b) parallel to the vector joining the centers of the monomer segments.

Having seen that the SAFT-VR+D equation can accurately describe the fluid phase behavior of dipolar square-well monomer fluids, we now turn to dipolar chain molecules. We first focus on diatomic molecules with a dipole moment in the center of both segments. In the SAFT-VR+D approach, the relative orientation of each dipole moment can be specifically determined by the azimuthal θ and polar ϕ angles of the intersegment axis (Fig. 1). Here we consider two specific diatomic molecules in which the dipole moments are both oriented perpendicular and parallel to the vector joining the centers of the monomers, as illustrated in Figs. 6(a) and 6(b). Since the radial distribution function is dependent on the relative orientation of the dipole moments, here we are examining the ability of the theory to capture the effect of dipole orientation on the phase behavior of dipolar chain molecules. In Fig. 7 we present the *PVT* behavior for dipolar square-well diatomic fluids which have the same model parameters ($\varepsilon^*=1.0$, $\lambda=1.5$, $\sigma^*=1.0$, and $\mu^{*2}=0.5$) in

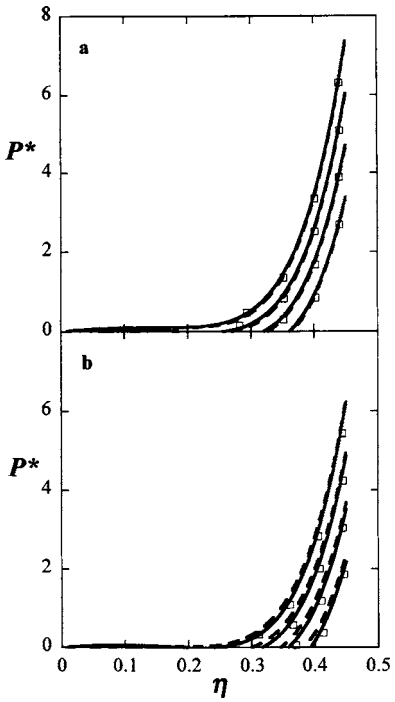

FIG. 7. Isotherms for dipolar square-well diatomic fluids with $\varepsilon^*=1.0$, $\lambda=1.5$, $\sigma^*=1.0$, and dipole moments $\mu^{*2}=0.5$ (a) perpendicular at $T^*=1.2$, 1.4, 1.6, and 1.8 (from bottom to top) and (b) parallel at $T^*=1.0$, 1.2, 1.4, and 1.6. The squares represent MC simulation results, the solid lines predictions from the SAFT-VR+D equation with the LEXP approximation, and the dashed lines from SAFT-VR+D approach with the GMSA approximation.

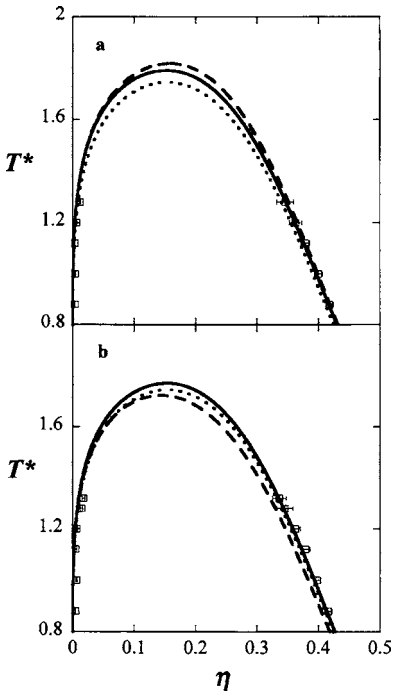

FIG. 8. Coexisting densities of dipolar square-well diatomic fluids with $\varepsilon^*=1.0$, $\lambda=1.5$, $\sigma^*=1.0$, and dipole moments $\mu^{*2}=0.5$ (a) perpendicular and (b) parallel. The squares represent MC simulation results, the solid lines predictions from the SAFT-VR+D equation with the LEXP approximation, the dashed lines from the SAFT-VR+D equation with the GMSA approximation, and the dotted lines predictions from the SAFT-VR+D equation for $\mu^{*2}=0$.

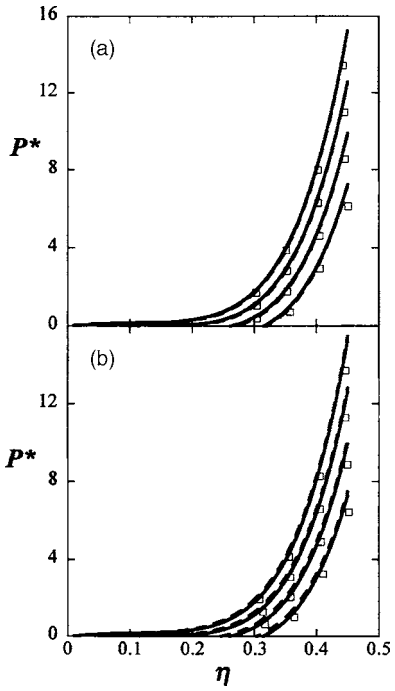

FIG. 9. Isotherms for dipolar square-well (SW) diatomic fluids with $\varepsilon^*=1.0$, $\lambda=1.8$, $\sigma^*=1.0$, and dipole moments $\mu^{*2}=0.5$ (a) perpendicular at $T^*=2.0$, 2.4, 2.8, and 3.2 (from bottom to top) and (b) parallel at $T^*=2.0$, 2.4, 2.8, and 3.2. The squares represent MC simulation results, the solid lines predictions from the SAFT-VR+D equation with the LEXP approximation, and the dashed lines from the SAFT-VR+D equation with the GMSA approximation.

each segment, but in (a) the dipole moments are aligned perpendicularly and in (b) they are aligned in parallel. The corresponding phase envelopes are presented in Fig. 8. From the figures, we find that the fluids with the dipole moments aligned in parallel exhibit a slightly higher density at a given pressure and temperature, and a slightly lower critical temperature, than the fluids in which the dipoles are perpendicularly aligned. We find that the SAFT-VR+D EOS with the GMSA provides good agreement with the simulation data for the isotherms studied and the coexisting densities of the dipolar diatomic fluid with dipole moments in the perpendicular (system 6) arrangement. However, for the dipolar diatomic fluid in which the dipole moments are aligned in parallel (system 5), the SAFT-VR+D EOS with the GMSA approximation underpredicts the density at a given pressure and temperature compared with the *NPT* ensemble simulations, particularly at low densities, and underestimates the saturated liquid density compared with the GEMC simulations. We believe that the main reason for the observed deviation is that, as stated earlier, Wertheim's solution for dipolar hard spheres with the MSA closure underestimates the radial distribution function for dipolar fluids at contact. If the GMSA is replaced by the LEXP approximation in the SAFT-VR+D EOS, a significant improvement in the theoretical predictions in comparison with the simulation data is seen (Figs. 7 and 8) for both the *PVT* and phase behavior. This result confirms that an accurate description of the fluid structure is very important in determining the thermodynamic properties of chain fluids. We have also studied the *PVT* behavior of the parallel and perpendicularly aligned dipolar diatomic fluids with $\lambda=1.8$ (systems 7 and 8), the results of which are presented in Fig. 9. Again we observe that the SAFT-VR+D EOS with the LEXP approximation provides good agreement with the simulation data for fluids with the dipole moments arranged perpendicularly and in parallel, while the use of the GMSA results in significant deviations for the fluids in which the dipolar segments are aligned in parallel. The SAFT-VR+D equation is therefore able to capture both the effect of potential range and orientation of the dipolar interactions on the phase behavior.

Since real fluids, such as ketones, alcohols, and many polymers, are typically composed of a mixture of polar and nonpolar groups, it is desirable to be able to model chain molecules comprised of segments that have different magnitudes and orientations of dipole moments. To this end, we have studied the *PVT* behavior of dipolar diatomic fluids with different dipole moments in each segment (systems 9 and 10). In particular, we have studied diatomics in which the magnitude of the dipole in one segment is twice that of the other segment [Fig. 10(a) and 10(b)], the results of which for perpendicular and parallel orientations of the dipoles are shown in Figs. 11(a) and 11(b), respectively. We again find that the SAFT-VR+D approach with the LEXP approxima-

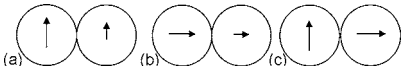

FIG. 10. Schematic showing the diatomic molecular models used to describe a chain fluid with different magnitude and orientation of dipole moments embedded in the center of each segment.

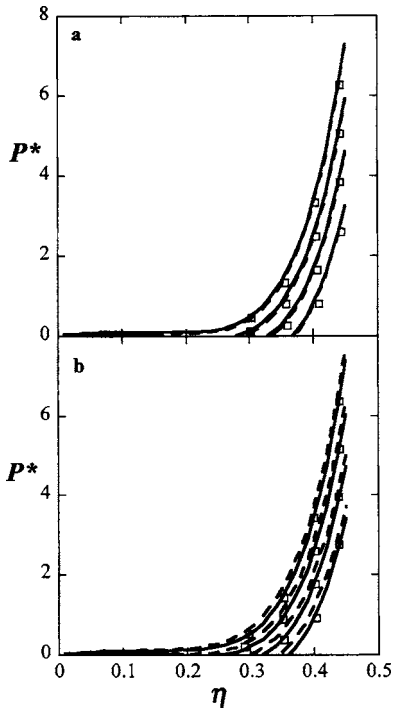

FIG. 11. Isotherms for dipolar square-well diatomic fluids with $\varepsilon^*=1.0$, $\lambda=1.5$, and $\sigma^*=1.0$ at $T^*=1.0$, 1.2, 1.4, and 1.6 with (a) perpendicular dipole moments of $\mu_1^{*2}=1.0$ and $\mu_2^{*2}=0.5$ and (b) parallel dipole moments of $\mu_1^{*2}=1.0$ and $\mu_2^{*2}=0.5$. The squares represent MC simulation results, the solid lines predictions from the SAFT-VR+D equation with the LEXP approximation, and the dashed lines from the SAFT-VR+D equation with the GMSA approximation.

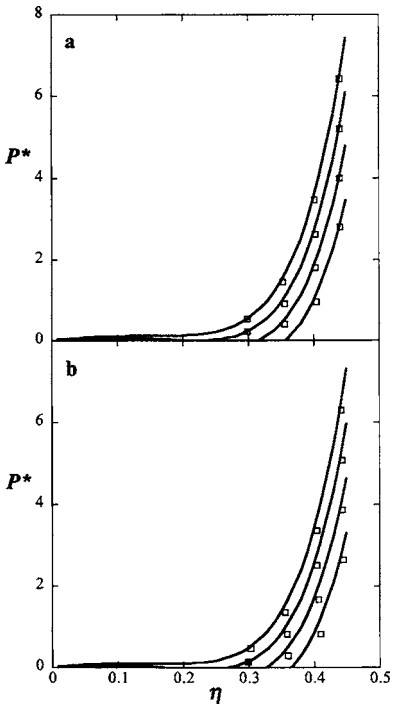

FIG. 12. Isotherms for dipolar square-well diatomic fluids with $\varepsilon^*=1.0$, $\lambda=1.5$, $\sigma^*=1.0$, and (a) perpendicular dipole moments of $\mu_1^{*2}=0.5$ and parallel dipole moments of $\mu_2^{*2}=0.5$ at $T^*=1.0$, 1.2, 1.4, and 1.6. (b) perpendicular dipole moment of $\mu_1^{*2}=1.0$ and parallel dipole moment of $\mu_2^{*2}=1.0$ at $T^*=1.0$, 1.2, 1.4, and 1.6. The squares represent MC simulation results, and the solid lines predictions from the SAFT-VR+D equation with the LEXP approximation.

tion provides good agreement with the simulation data for diatomic fluids with different magnitudes of dipole moments arranged both perpendicularly and in parallel. However, again, the SAFT-VR+D approach with the GMSA approximation underestimates the densities at a given pressure and temperature for the molecule with the dipole moments arranged perpendicularly. We have also studied the *PVT* behavior of diatomic dipolar fluids with different orientations of dipole moments in each segment (systems 11 and 12), as shown in Fig. 10(c). In these fluids, the pair distribution function due to the dipolar interaction will vanish since the angle-related functions $\Delta(\mathbf{n}_1\mathbf{n}_2)$ and $D(\mathbf{n}_1\mathbf{n}_2\hat{\mathbf{r}})$ in Eq. (15) are zero for the 90° relative orientation of the two dipoles [Fig. 10(c)]. In this case, the predictions from the SAFT-VR+D approach with the LEXP approximation and the GMSA approximation are the same. From Fig. 12, we note that in all cases, good agreement is observed between the predictions from the SAFT-VR+D approach and simulation data, indicating that the theory can accurately describe the thermodynamic and phase behavior of fluids composed of segments with differing dipole moments.

To illustrate the generality of this approach, we have also studied a model triatomic fluid in which the dipole moments are arranged perpendicularly or in parallel in the first two segments, with the third segment having no dipole moment (Fig. 13). Within the solution of Adelman and Deutch[30] for polar mixtures with the MSA closure, the SAFT-VR+D EOS describes a molecule consisting of a mixture of nondipolar and dipolar segments with an effective dipole moment and density for the dipolar interaction. As mentioned before, due to the linearity in the MSA approximation, the anisotropic contribution to the pair distribution function due to the dipolar interaction between dipolar segments and nondipolar segments equals zero. In the SAFT-VR+D approach, the pair distribution function between dipolar square-well segments and nondipolar square-well segments is therefore equivalent to that between nondipolar square-well segments. In the case of the triatomic molecules shown in Fig. 13, the pair distribution function between segments 1 and 2 is $g^{\mathrm{DSW}}(\mathbf{r}\boldsymbol{\omega}_1\boldsymbol{\omega}_2)$ and the pair distribution function between segments 2 and 3 is $g_{23}^{\mathrm{SW}}(\mathbf{r})$. The Helmholtz free energy due to chain formation is therefore given by Eq. (41), in which the total number of segments is 3 and the number of pairs of dipolar segments is 1. This approach therefore describes a heteronuclear fluid, as the chain is composed of unlike segments, and can be modeled as in our previous work.[44] In Fig. 14 we present isotherms predicted from the SAFT-VR+D approach compared to *NPT* MC simulation data for two triatomic fluids (systems 13 and 14) with $\epsilon^*=1.0$, $\lambda=1.5$, $\sigma^*=1.0$, and reduced dipole moments of $\mu^{*2}=1.0$ in both segments and arranged in parallel (system 13) and perpendicularly (system 14). We find that the fluid with the dipole mo-

FIG. 13. Schematic illustrating the triatomic molecular model used to describe a chain fluid with dipole moments embedded in the center of the first two segments. Segments are labeled 1–3 from left to right.

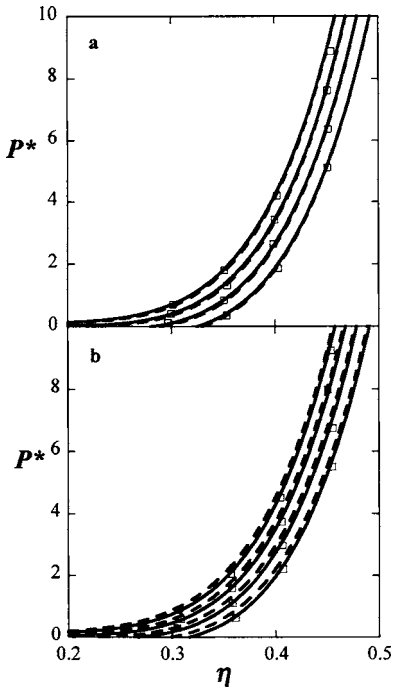

FIG. 14. Isotherms for dipolar square-well triatomic fluids with $\varepsilon^*=1.0$, $\lambda=1.5$, $\sigma^*=1.0$, and dipole moments $\mu^{*2}=1.0$ (a) perpendicular and (b) parallel at $T^*=1.6$, 1.8, 2.0, and 2.2 (from bottom to top). The squares represent MC simulation results, the solid lines predictions from the SAFT-VR+D equation with the LEXP approximation, and the dashed lines from the SAFT-VR+D equation with the GMSA approximation.

ments in the parallel arrangement has a slightly higher pressure than the fluid with dipole moments arranged perpendicularly at given density and temperature, when all other parameters are the same. Good agreement is observed between the predictions from the SAFT-VR+D approach with the GMSA approximation and simulation data for system 14 in which the dipole moments are aligned perpendicularly, while the SAFT-VR+D EOS with the LEXP approximation again provides excellent predictions for both fluids. Hence the solution of Adelman and Deutch when combined with the hetero-SAFT-VR approach is able to accurately predict thermodynamic properties for dipolar square-well chain fluids consisting of dipolar and nondipolar segments.

V. CONCLUSIONS

In this work, a SAFT-VR-like approach, SAFT-VR+D, has been developed to study dipolar chain fluids which takes the dipolar square-well fluid as the reference state. In this way, the SAFT-VR+D approach explicitly takes into account the magnitude and orientation of dipole moments, all of which are found to affect the thermodynamics and phase behavior of dipolar square-well monomer and chain fluids. In order to gain a comprehensive understanding of the thermodynamic properties of the systems studied, and validate the SAFT-VR+D approach, both *NPT* MC and GEMC simulations were performed to obtain simulation data to compare to the theoretical predictions. We found that the SAFT-VR+D equation with the GMSA approximation provides good predictions for the phase behavior of the dipolar monomer fluids studied and of chain fluids with a perpendicular arrangement of the dipole moments. A more accurate approximation for the radial distribution function of dipolar square-well fluids (LEXP approximation) was implemented to improve the performance of the SAFT-VR+D EOS for dipolar chain fluids in which the dipole moments are parallel to the vector joining the centers of the monomers. It is found that the SAFT -VR+D equation with the LEXP approximation is suitable for fluids with both vertical and horizontal arrangements of the dipole moments. Furthermore, using the solution of Adelman and Deutch for polar mixtures, the SAFT-VR+D with LEXP approximation gives a good description of the thermodynamic properties of dipolar chain fluids consisting of nondipolar segments and dipolar segments. In future work, the SAFT-VR+D approach will be applied to study real fluids and their mixtures.

ACKNOWLEDGMENTS

We gratefully acknowledge financial support from the National Science Foundation under Grant No. CTS-0452688. We would also like to thank Peter Cummings for useful discussions.

[1] W. G. Chapman, K. E. Gubbins, G. Jackson, and M. Radosz, Fluid Phase Equilib. **52**, 31 (1989); Ind. Eng. Chem. Res. **29**, 1709 (1990).
[2] M. S. Wertheim, J. Stat. Phys. **35**, 19 (1984); **35**, 35 (1984); **42**, 459 (1986); **42**, 477 (1986).
[3] I. G. Economou, Ind. Eng. Chem. Res. **41**, 953 (2002).
[4] A. Gil-Villegas, A. Galindo, P. J. Whitehead, S. J. Mills, G. Jackson, and A. N. Burgess, J. Chem. Phys. **106**, 4168 (1997).
[5] A. Galindo, L. A. Davies, A. Gil-Villegas, and G. Jackson, Mol. Phys. **93**, 241 (1998).
[6] C. McCabe and G. Jackson, Phys. Chem. Chem. Phys. **1**, 2057 (1999); C. McCabe, A. Galindo, M. N. Garcia-Lisbona, and G. Jackson, Ind. Eng. Chem. Res. **40**, 3835 (2001); C. McCabe and S. B. Kiselev, Fluid Phase Equilib. **219**, 3 (2004); Ind. Eng. Chem. Res. **43**, 2839 (2004).
[7] C. McCabe, A. Galindo, A. Gil-Villegas, and G. Jackson, Int. J. Thermophys. **19**, 1511 (1998); C. McCabe, A. Gil-Villegas, and G. Jackson, J. Phys. Chem. B **102**, 4183 (1998); A. Galindo, L. J. Florusse, and C. J. Peters, Fluid Phase Equilib. **160**, 123 (1999); E. J. M. Filipe, E. de Azevedo, L. F. G. Martins, V. A. M. Soares, J. C. G. Calado, C. McCabe, and G. Jackson, J. Phys. Chem. B **104**, 1315 (2000); E. J. M. Filipe, L. F. G. Martins, J. C. G. Calado, C. McCabe, and G. Jackson, *ibid.* **104**, 1322 (2000); E. J. M. Filipe, L. M. B. Dias, J. C. G. Calado, C. McCabe, and G. Jackson, Phys. Chem. Chem. Phys. **4**, 1618 (2002); L. M. B. Dias, E. J. M. Filipe, C. McCabe, and J. C. G. Calado, J. Phys. Chem. B **108**, 7377 (2004); L. X. Sun, H. G. Zhao, S. B. Kiselev, and C. McCabe, *ibid.* **109**, 9047 (2005).
[8] L. X. Sun, H. G. Zhao, S. B. Kiselev, and C. McCabe, Fluid Phase Equilib. **228**, 275 (2005).
[9] C. McCabe, A. Galindo, A. Gil-Villegas, and G. Jackson, J. Phys. Chem. B **102**, 8060 (1998); R. P. Bonifacio, E. J. M. Filipe, C. McCabe, M. F. C. Gomes, and A. A. H. Padua, Mol. Phys. **100**, 2547 (2002); P. Morgado, C. McCabe, and E. J. M. Filipe, Fluid Phase Equilib. **228**, 389 (2005).
[10] F. J. Blas and A. Galindo, Fluid Phase Equilib. **194–197**, 501 (2002).
[11] L. M. B. Dias, R. P. Bonifacio, E. J. M. Filipe, J. C. G. Calado, C. McCabe, and G. Jackson, Fluid Phase Equilib. **205**, 163 (2003).
[12] C. McCabe, A. Galindo, and P. T. Cummings, J. Phys. Chem. B **107**, 12307 (2003); A. Valtz, A. Chapoy, C. Coquelet, P. Paricaud, and D. Richon, Fluid Phase Equilib. **226**, 333 (2004).
[13] A. Galindo, A. Gil-Villegas, P. J. Whitehead, G. Jackson, and A. N. Burgess, J. Phys. Chem. B **102**, 7632 (1998).
[14] A. Galindo and F. J. Blas, J. Phys. Chem. B **106**, 4503 (2002); C. M. Colina, A. Galindo, F. J. Blas, and K. E. Gubbins, Fluid Phase Equilib. **222**, 77 (2004); C. M. Colina and K. E. Gubbins, J. Phys. Chem. B **109**, 2899 (2005).
[15] A. Galindo, A. Gil-Villegas, G. Jackson, and A. N. Burgess, J. Phys. Chem. B **103**, 10272 (1999); A. Gil-Villegas, A. Galindo, and G. Jack-

son, Mol. Phys. **99**, 531 (2001); B. H. Patel, P. Paricaud, A. Galindo, and G. C. Maitland, Ind. Eng. Chem. Res. **42**, 3809 (2003); B. Behzadi, B. H. Patel, A. Galindo, and C. Ghotbi, Fluid Phase Equilib. **236**, 241 (2005).
[16] T. Kraska and K. E. Gubbins, Ind. Eng. Chem. Res. **35**, 4727 (1996); **35**, 4738 (1996).
[17] E. A. Muller and K. E. Gubbins, Ind. Eng. Chem. Res. **34**, 3662 (1995).
[18] K. Xu, Y. G. Li, and W. B. Liu, Fluid Phase Equilib. **142**, 55 (1998).
[19] K. E. Gubbins and C. G. Gray, Mol. Phys. **23**, 187 (1972).
[20] G. Stell, J. C. Rasaiah, and H. Narang, Mol. Phys. **23**, 393 (1972).
[21] P. K. Jog and W. G. Chapman, Mol. Phys. **97**, 307 (1999); P. K. Jog, S. G. Sauer, J. Blaesing, and W. G. Chapman, Ind. Eng. Chem. Res. **40**, 4641 (2001).
[22] F. Tumakaka and G. Sadowski, Fluid Phase Equilib. **217**, 233 (2004).
[23] A. Dominik, W. G. Chapman, M. Kleiner, and G. Sadowski, Ind. Eng. Chem. Res. **44**, 6928 (2005).
[24] B. Saager, J. Fischer, and M. Neumann, Mol. Simul. **8**, 27 (1991); B. Saager and J. Fischer, Fluid Phase Equilib. **72**, 67 (1992).
[25] J. Gross and J. Vrabec, AIChE J. **52**, 1194 (2006).
[26] M. S. Wertheim, J. Chem. Phys. **55**, 4291 (1971).
[27] G. N. Patey and J. P. Valleau, J. Chem. Phys. **61**, 534 (1974).
[28] L. Verlet and J. J. Weis, Mol. Phys. **28**, 665 (1974).
[29] H. C. Andersen, D. Chandler, and J. D. Weeks, J. Chem. Phys. **56**, 3812 (1972).
[30] S. A. Adelman and J. M. Deutch, J. Chem. Phys. **59**, 3971 (1973).
[31] P. H. Fries and G. N. Patey, J. Chem. Phys. **82**, 429 (1985); J. S. Perkyns, P. H. Fries, and G. N. Patey, Mol. Phys. **57**, 529 (1986); P. H. Lee and B. M. Ladanyi, J. Chem. Phys. **91**, 7063 (1989).
[32] C. G. Gray and K. E. Gubbins, *Theory of Molecular Fluids* (Clarendon, Oxford, 1984).
[33] J. S. Hoye, J. L. Lebowitz, and G. Stell, J. Chem. Phys. **61**, 3253 (1974); G. Stell and S. F. Sun, J. Chem. Phys. **63**, 5333 (1975).
[34] A. Gil-Villegas, A. Galindo, P. J. Whitehead, S. J. Mills, G. Jackson, and A. N. Burgess, J. Chem. Phys. **106**, 4168 (1997).
[35] Y. Peng, H. Zhao, and C. McCabe, Mol. Phys. **104**, 571 (2006).
[36] C. G. Gray, Y. S. Sainger, C. G. Joslin, P. T. Cummings, and S. Goldman, J. Chem. Phys. **85**, 1502 (1986).
[37] J. A. Barker and R. O. Watts, Mol. Phys. **26**, 789 (1973); P. Cummings, I. Nezbeda, W. R. Smith, and G. Morriss, *ibid.* **43**, 1471 (1981); A. Gil-Villegas, G. Jackson, and S. C. McGrother, J. Mol. Liq. **76**, 171 (1998).
[38] A. L. Benavides, Y. Guevara, and F. Delrio, Physica A **202**, 420 (1994).
[39] B. Garzon, S. Lago, and C. Vega, Chem. Phys. Lett. **231**, 366 (1994).
[40] B. Smith, C. P. Williams, E. M. Hendriks, and S. W. Deleeuw, Mol. Phys. **68**, 765 (1989).
[41] See EPAPS Document No. E-JCPSA6-125-504634 for tables of the numerical results from the molecular simulations performed in this work. This document can be reached via a direct link in the online article's HTML reference section or via the EPAPS homepage (http:www.aip.org/pubservs/epaps.html).
[42] J. V. Sengers and J. M. H. Levelt Sengers, Annu. Rev. Phys. Chem. **37**, 189 (1986).
[43] A. Gil-Villegas, A. Galindo, P. J. Whitehead, S. J. Mills, and G. Jackson, J. Chem. Phys. **106**, 4168 (1997).
[44] Y. Peng, H. G. Zhao, and C. McCabe, Mol. Phys. **104**, 571 (2006).